

# Structure and Magnetic Properties of Oxide Nanoparticles of Fe-Co-Ni Synthesized by Co-Precipitation Method

A. Ghasemi<sup>1</sup>, A. M. Davarpanah<sup>1</sup>, M. Ghadiri<sup>2\*</sup>

1- Department of Physics, Faculty of Science, University of Sistan and Baluchestan, Zahedan, I. R. Iran

2- Chemical Engineering Department, Urmia University of Technology ( UUT), Urmia , I. R. Iran

(\*) Corresponding author: m.ghadiri@uut.ac.ir

(Received: 13 Oct. 2012 and Accepted: 28 Dec. 2012)

## Abstract:

Oxide nanoparticles of Fe-Co-Ni were prepared in six different compositions by co-precipitation method. The as-synthesized nanoparticles were characterized by X-Ray Diffraction (XRD), Field Emission Scanning Electron microscope (FESEM), Fourier Transform Infrared (FT-IR) and Vibrating Sample Magnetometer (VSM). It was found that the nanoparticles had mean crystalline size of 30-55 nm and spherical shape. Specific surface area of the nanoparticles was between  $27.47 \times 10^4 \text{ cm}^2/\text{g}$  to  $141.4 \times 10^4 \text{ cm}^2/\text{g}$  which had been calculated by X-Ray Diffraction data. The magnetic measurements of nanoparticles were done at room temperature and found that nanoparticles exhibit a ferromagnetic behavior with different values of saturation magnetization and coercivity.

**Keywords:** Nanostructured materials, Precipitation, X-ray diffraction, Magnetic measurements, Nanoparticles.

## 1. INTRODUCTION

Synthesis and application of nanomaterials is the subject of most researches because of their unique physical and chemical properties, which make them very interesting in view of both, the scientific value of understanding their properties and the technological significance of enhancing the performance of existing materials [1-10]. Magnetic properties of nano-scale materials are used in high density recording, color imaging, ferro fluid, high frequency devices, magnetic refrigerators and so on [11-12].

Several methods for synthesis of nanoparticles have been developed during this decade and it becomes easy now to prepare ceramic nanoparticles [13]. However, research on oxide nanoparticles of metallic alloys is very few. A few methods have been reported on the preparation of Fe-Co-Ni ternary alloys and also their oxide such as hydrogen plasma-metal

reaction [13] and mechanical synthesis [14-15]. In the present contribution, several types of oxide nanoparticles of Fe-Co-Ni were synthesized by co-precipitation method. Compared to conventional methods, it does not need advanced instruments. To the best our knowledge, this is the first report on the synthesis oxide of Fe-Co-Ni by co-precipitation method. The aim of the present work is to prepare oxide nanoparticles Fe-Co-Ni using co-precipitation method and its physicochemical characterization.

## 2. EXPERIMENTAL

### 2.1. Synthesis

Co-precipitation method was used to prepare 6 types of oxide nanoparticles,  $\text{Fe}_{20}\text{Co}_{20}\text{Ni}_{60}\text{O}_x$ ,  $\text{Fe}_{40}\text{Co}_{20}\text{Ni}_{40}\text{O}_x$ ,  $\text{Fe}_{60}\text{Co}_{20}\text{Ni}_{20}\text{O}_x$ ,  $\text{Fe}_{20}\text{Co}_{40}\text{Ni}_{40}\text{O}_x$ ,  $\text{Fe}_{40}\text{Co}_{40}\text{Ni}_{20}\text{O}_x$  and  $\text{Fe}_{20}\text{Co}_{60}\text{Ni}_{20}\text{O}_x$  (at %), which were labeled as a, b, c, d, e and f, respectively.  $\text{Ni}(\text{NO}_3)_2 \cdot 6\text{H}_2\text{O}$ ,  $\text{Co}(\text{NO}_3)_2 \cdot 6\text{H}_2\text{O}$  and  $\text{Fe}(\text{NO}_3)_3 \cdot 9\text{H}_2\text{O}$

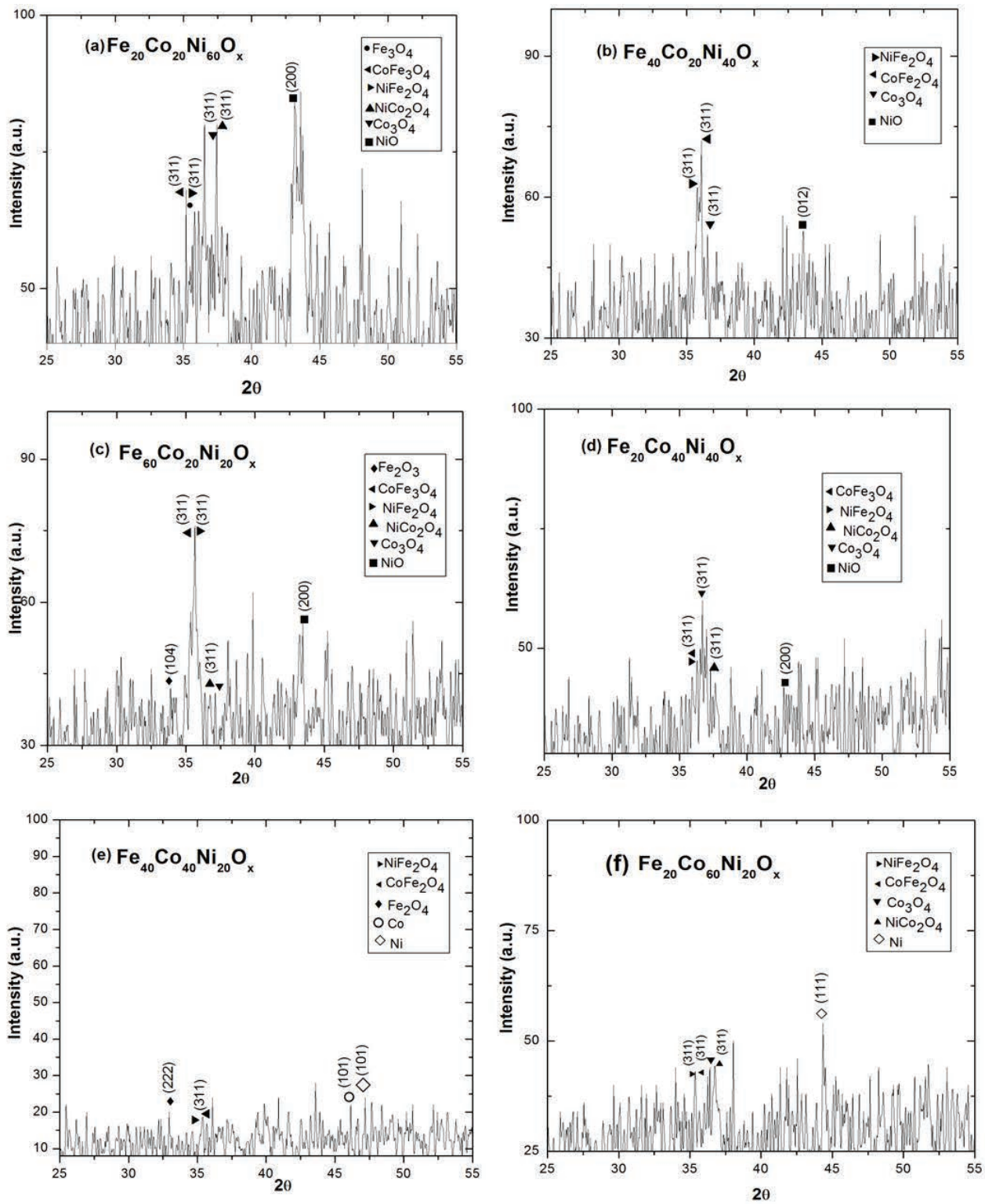


Figure 1: The XRD patterns of the synthesized samples.

as precursors were obtained from MERCK and used without any further purification. Firstly, 2M solutions of all precursors were prepared with doubly distilled water. The sediment formed under water bath conditions at about 70°C was washed using first with 1L of boiling and then with 1L of cold doubly distilled water. We used 2M solution of Sodium carbonate (Na<sub>2</sub>CO<sub>3</sub>) as precipitant agent under water bath conditions. Washed sediment was dried in an oven at about 115°C for 12h. Finally, the products were calcined at 600°C for 6h.

## 2.2. Characterization

Investigations on morphology of the compositions were carried out using a Field Emission Scanning Electron Microscope (FESEM, HITACHI-Japan S4160) operated at 15.0 kV. The X-Ray Diffraction analysis was done by X-Ray Diffraction (XRD, GNR- MPD 3000) at a scanning rate of 0.02° .S<sup>-1</sup> in the range of 2θ= 25–55°, using Cu Kα radiation (λ = 1.5406 Å ). FT-IR (JASCO FT/IR-460plus) has been used to obtain the formation of the nanoparticles from the precursors. The magnetic properties were assessed with a Vibrating Sample Magnetometer (IRAN/VSM-4inch) at room temperature.

## 3. RESULTS AND DISCUSSION

The XRD patterns of the as-synthesized samples

are shown in Figure 1. The samples have a FCC and mixture of FCC and Rhombohedral structure and also a mixture of FCC, BCC and Hexagonal structure. According to the XRD patterns, the samples are mostly composed of spinel structure with chemical formula of AB<sub>2</sub>O<sub>4</sub>. It is considerable that the position of the strongest peak relevant to each of the phase structure has just been shown in the patterns.

The crystallite size of the samples was estimated by Debye-Scherrer equation [16]:

$$D = \frac{0.9\lambda}{\beta \cos\theta} \quad (1)$$

Where λ, β and θ are the X-Ray wavelength, the full width at half maximum (FWHM) of the diffraction peak and the Bragg diffraction angle, respectively. The calculated crystallite size shown in Table 1 lies in the range of 30-55 nm.

The specific areas of the samples, calculated by the equation 2, are shown in Table 1 [17]:

$$S_a = \frac{6}{DD_x} \quad (2)$$

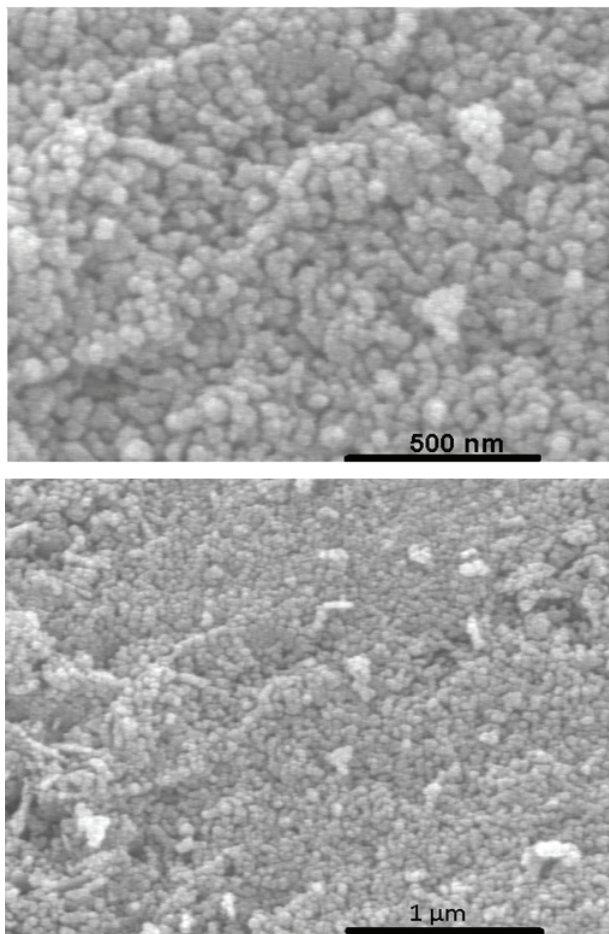
Where D and D<sub>x</sub> are particle size and X-Ray density of the phase structure in each sample, respectively. The estimated values of specific surface area lie in the range of 27.46x10<sup>4</sup> to 141.4x10<sup>4</sup> cm<sup>2</sup>/g.

Figure 2 shows FESEM images of the Fe<sub>60</sub>Co<sub>20</sub>Ni<sub>20</sub>O<sub>x</sub> sample. According to images, nanoparticles

**Table 1:** phase constitution, specific surface area and crystallite size of the as-synthesized samples.

Samples	Phase constitution	Specific surface area (cm <sup>2</sup> /g)	Crystallite size (nm)
Fe <sub>20</sub> Co <sub>20</sub> Ni <sub>60</sub> O <sub>x</sub>	FCC	141.4 × 10 <sup>4</sup>	30
Fe <sub>40</sub> Co <sub>20</sub> Ni <sub>40</sub> O <sub>x</sub>	FCC	86.2 × 10 <sup>4</sup>	55
	Rhombohedral		
Fe <sub>60</sub> Co <sub>20</sub> Ni <sub>20</sub> O <sub>x</sub>	FCC	84.1 × 10 <sup>4</sup>	32
	Rhombohedral		
Fe <sub>20</sub> Co <sub>40</sub> Ni <sub>40</sub> O <sub>x</sub>	FCC	59 × 10 <sup>4</sup>	48
Fe <sub>40</sub> Co <sub>40</sub> Ni <sub>20</sub> O <sub>x</sub>	FCC	27.46 × 10 <sup>4</sup>	33
	BCC		
	Hexagonal		
Fe <sub>20</sub> Co <sub>60</sub> Ni <sub>20</sub> O <sub>x</sub>	FCC	88.52 × 10 <sup>4</sup>	39

synthesized possess nearby spherical shape. The FT-IR spectra of the sediments dried at 115°C have been shown in Figure 3. Because of the presence of carbonate ion in samples, stretch vibration bonds of C–O and C=O have been appeared as an impurity in the range of 1355–1396 $\text{cm}^{-1}$  and 1633 $\text{cm}^{-1}$ , respectively. As shown in this figure, absorption bond at 3446 $\text{cm}^{-1}$  is corresponding to the O–H stretching vibrations in the samples [18].



**Figure 2:** FESEM images of (c) sample.

Figure 4 shows the FT-IR spectra of the samples calcined at 600°C. As shown in table 2, the spectra display that stretch vibration bonds of C=O and C–O have been removed in all of compounds and bonds related to the metal–oxygen stretching vibration have been appeared [18-21].

Figure 5 shows the hysteresis loops measured at room temperature by VSM for the samples. All the samples are ferromagnetic. Table 3 shows that

the Fe-rich sample has the most value of saturation magnetization, remanent magnetization and coercivity. With increasing Ni content  $M_s$ ,  $M_r$  and  $H_c$  decrease and finally the Co-rich sample has least  $M_s$  and  $M_r$ . Li et al. [13] have reported higher values of  $H_c$  and  $M_s$  for the oxide compositions. Different values of  $M_s$  and  $H_c$  is due to the preparation process.

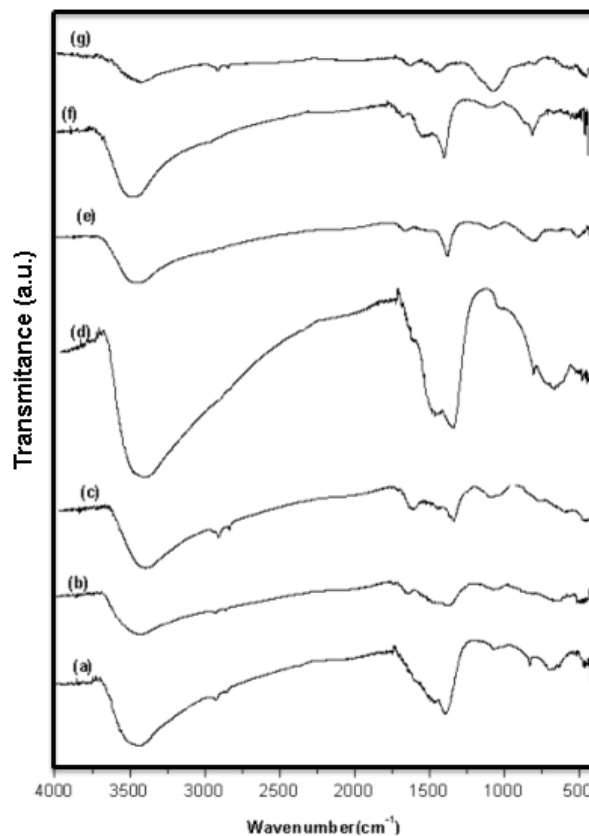


**Figure 3:** The FT-IR spectra of the all sample dried at 115 °C. The spectrum of the (g) sample is relevant to KBr

Oxide samples synthesized by hydrogen plasma-metal reaction were acicular [13]. In this work, according to FESEM images, the samples possess nearby spherical shape. According to the literature [13], the shape magnetic anisotropy is usually more important in the transition alloys, so the lower value of  $M_s$  and  $H_c$  may be due to the low shape magnetic anisotropy. Also, according to the literature [22], the  $M_s$  value increases with the enhancement of crystallinity, so the lower saturation magnetization is due to the lower crystallinity.

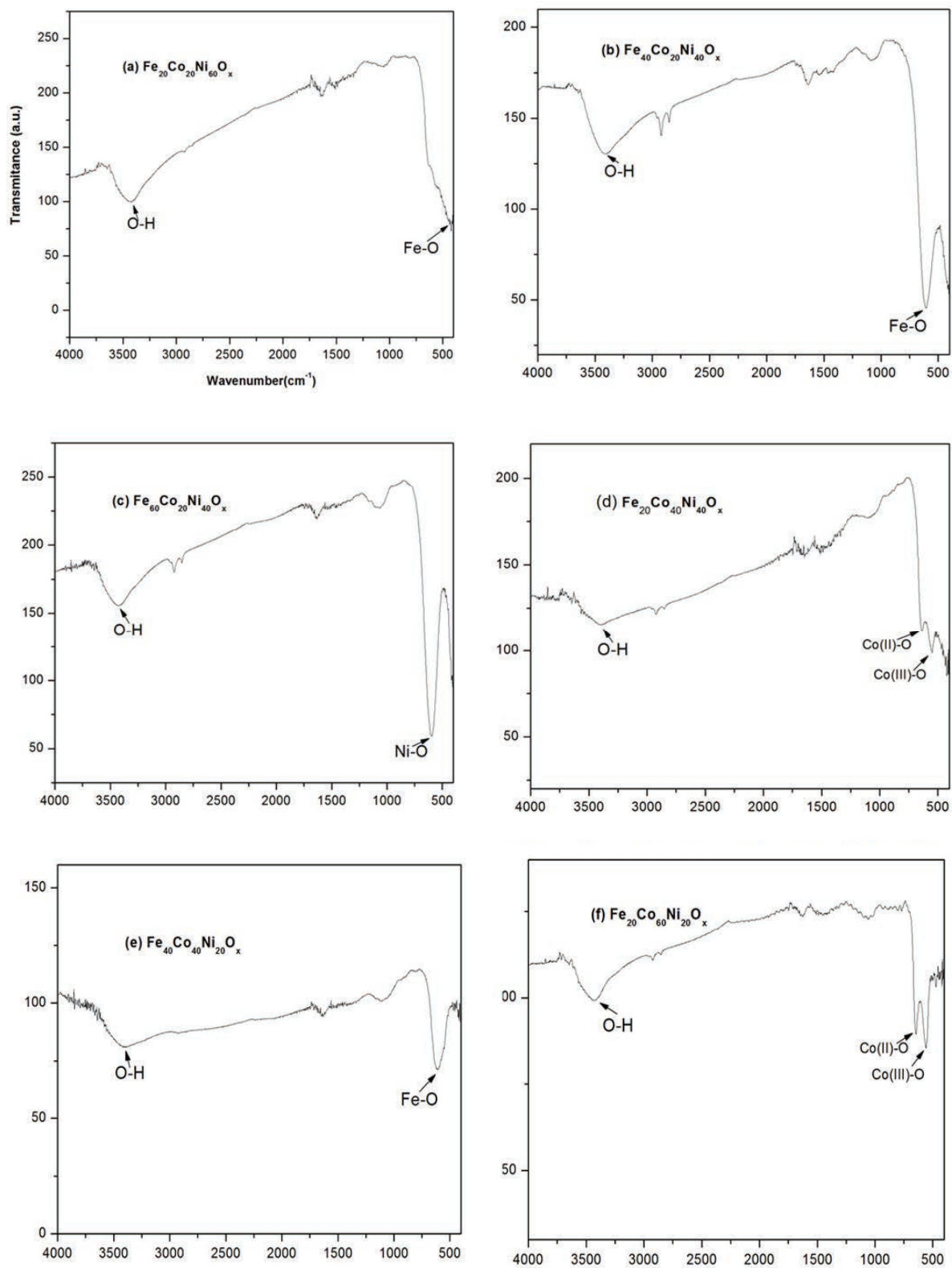


**Figure 4:** The FT-IR spectra of the calcined a-f samples.

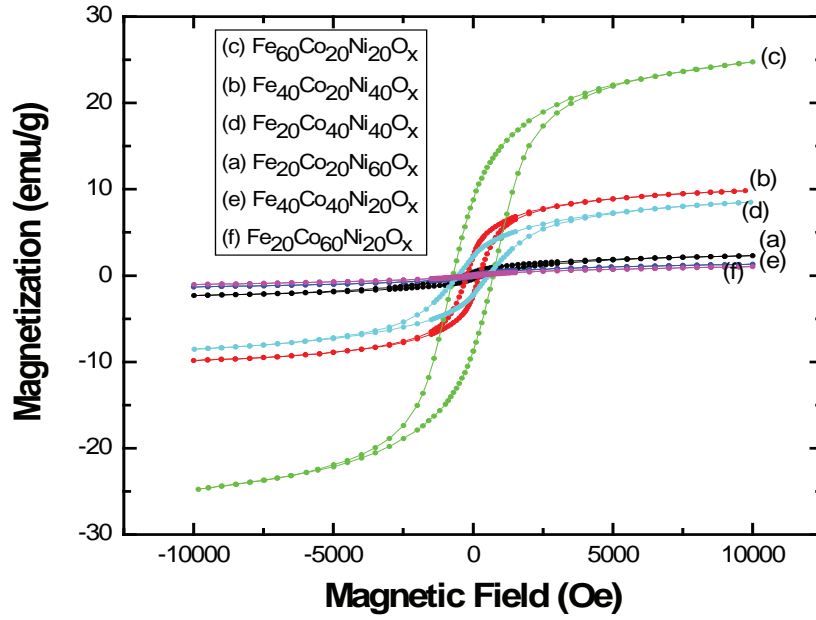


Figure 5: Hysteresis loops at 300K for six synthesized samples.

Table 2: The metal – oxygen bonds of synthesized samples appeared in the FT-IR spectra.

Samples	Fe – O (cm <sup>-1</sup> )	Ni – O (cm <sup>-1</sup> )	Co – O (cm <sup>-1</sup> )
(a)Fe <sub>20</sub> Co <sub>20</sub> Ni <sub>60</sub> O <sub>x</sub>	406	-	-
(b)Fe <sub>40</sub> Co <sub>20</sub> Ni <sub>40</sub> O <sub>x</sub>	607	-	-
(c)Fe <sub>60</sub> Co <sub>20</sub> Ni <sub>20</sub> O <sub>x</sub>	-	696	-
(d)Fe <sub>20</sub> Co <sub>40</sub> Ni <sub>40</sub> O <sub>x</sub>	-	-	549 Co(III) – O 636 Co(II) – O
(e)Fe <sub>40</sub> Co <sub>40</sub> Ni <sub>20</sub> O <sub>x</sub>	609	-	-
(f)Fe <sub>20</sub> Co <sub>60</sub> Ni <sub>20</sub> O <sub>x</sub>	-	-	644 Co(II) – O 552 Co(III) – O

Table 3: Magnetic properties of synthesized nanoparticles.

Samples	M <sub>s</sub> (emu/g)	M <sub>r</sub> (emu/g)	H <sub>c</sub> (Oe)
(c)	24.71	9.55	720.16
(b)	9.92	2.76	223.3
(d)	8.56	2.16	507.71
(a)	2.29	0.49	335.1
(e)	1.32	0.14	81.2
(f)	1.04	0.06	134.22

#### 4. CONCLUSIONS

The oxide nanoparticles of the Fe-Co-Ni have been synthesized by Co-precipitation method. According to XRD data, the compositions mostly include spinel structures and crystalline size of the samples was in the range of 30-55 nm. FESEM indicates that the nanoparticles have nearby spherical structure. Using VSM, it was clear that the samples have ferromagnetic behavior.

#### ACKNOWLEDGEMENTS

The authors would like to thank Prof. A.A. Mirzae from Department of Chemistry, University of Sistan and Baluchestan, Zahedan for technical supports of Chemistry laboratory.

#### REFERENCES

1. M. Khatamian, A. A. Khandar, M. Haghghi, M. Ghadiri, M. Darbandi, Powder Technol. Vol. 203, (2010), pp. 503-509.
2. M. Khatamian, A.A. Khandar, M. Haghghi, M. Ghadiri, Appl. Surf. Sci. Vol. 258, (2011), pp. 865-872.
3. A.E. Strevens, A. Drury, S. M. Lipson, M. Kroll, W.J. Blau, H.H. Horhold, Appl. Phys. Lett. Vol. 86, (2005), p. 143503.
4. X. Yang, J. Dong, Appl. Phys. Lett. Vol. 86, (2005), p. 163105.
5. M. Endo, H. Muramatsu, T. Hayashi, Y. A. Kim, M. Terrones, M. S. Dresselhaus, Nature, Vol. 433, (2005), p. 476.
6. H. Cui, X. Yang, L. R. Baylor, D. H. Lowndes, Appl. Phys. Lett. Vol. 86, (2005), p. 053110.
7. S. Morup, C. Frandsen, Phys. Rev. Lett. Vol. 92, (2004), p. 217201.
8. O. Ozatay, P. Chalsani, N. C. Emloy, I. N. Krivorotov, R. A. Buhrman, J. Appl. Phys. Vol. 95, (2004), p. 7315.
9. F. Meier, V. Cerletti, O. Gywat, D. Loss, D. D Awschalom, Phys. Rev. Vol. B 69, (2004), p. 195315.
10. M. Srivastava, S. Chaubey, A. K. Ojha, Mater. Chem. Phys. Vol. 118, (2009), pp. 174-180.
11. J. L. Dorman, D. Fiorani (Eds.), Magnetic Properties of Fine Particles, North Holland, Amsterdam, 1992.
12. M. Kishimoto, Y. Sakurai, T. Ajima, J. Appl. Phys. Vol. 76, (1994), p. 7506.
13. X. Li, S. Takahashi, J. Magn. Magn. Mater. 214 (2000) 195-203.
14. A. Azizi, H. Yoozbashizadeh, S. K. Sadrnezhad, J. Magn. Magn. Mater. Vol. 321, (2009), pp. 2729-2732.
15. T. Pikula, L. Kubalova, D. Oleszak, J.K. Zurawicz, E. Jartych, J. Alloys Compd. Vol. 483, (2009), p. 582-584.
16. F. Davar, Z. Fereshteh, M. Salavati Niasari, J. Alloys Compd. Vol. 476, (2000), p. 797-801.
17. J. Pal, P. Chauhan, Mater. Charact, Vol. 61, (2010), p. 575-579.
18. A. S.Bhatt, D. K.Bhat, C. Tai, M. S.Santosh, Mater. Chem. Phys, Vol. 125, (2011), pp. 347-350.
19. M. Srivastava, A. Ojha, A. Materney, S. Chaubey, J. Alloys Compd, Vol. 481, (2009), pp. 515-519.
20. F. Davar, Z. Fereshteh, M. S.Niasari, J. Alloys Compd, Vol. 476, (2009), pp. 797-801.
21. W. Lu, Y. Shen, A. Xie, J. Magn. Magn. Mater, Vol. 322, (2010), pp. 1828-1833.
22. S. Maensiri, C. Masingboon, B. Banjong, S. Seraphin, J. Scripta Materialia, Vol. 56, (2007), pp. 797-800.

